

Optimal control of vaccination and plasma transfusion with potential usefulness for COVID-19*

Juliana Couras, Iván Area, Juan J. Nieto, Cristiana J. Silva and Delfim F. M. Torres

Abstract The SEIR model is a compartmental model used to simulate the dynamics of an epidemic. In this chapter, we introduce two control functions in the compartmental SEIR model representing vaccination and plasma transfusion. Optimal control problems are proposed to study the effects of these two control measures, on the reduction of infected individuals and increase of recovered ones, with minimal costs. Up to our knowledge, the plasma transfusion treatment has never been considered as a control strategy for epidemics mitigation. The proposed vaccination and treatment strategies may have a real application in the challenging and hard problem of controlling the COVID-19 pandemic.

Juliana Couras
University of Aveiro, 3810-193 Aveiro, Portugal, e-mail: julianacouras@ua.pt

Iván Area
Departamento de Matematica Aplicada II, E. E. Aeronautica e do Espazo, Campus de Ourense, Universidade de Vigo, 32004 Ourense, Spain e-mail: area@uvigo.es

Juan J. Nieto
Instituto de Matematicas, Universidade de Santiago de Compostela, 15782 Santiago de Compostela, Spain, e-mail: juanjose.nieto.roig@usc.es

Cristiana J. Silva
Center for Research and Development in Mathematics and Applications (CIDMA), Department of Mathematics, University of Aveiro, 3810-193 Aveiro, Portugal, e-mail: cjoasilva@ua.pt

Delfim F. M. Torres
Center for Research and Development in Mathematics and Applications (CIDMA), Department of Mathematics, University of Aveiro, 3810-193 Aveiro, Portugal, e-mail: delfim@ua.pt

* This is a preprint of a paper whose final and definite form is published in *Analysis of Infectious Disease Problems (Covid-19) and Their Global Impact*, Springer Nature Singapore Pte Ltd. Submitted 15/July/2020; revised 02/Oct/2020; accepted 08/Oct/2020.

1 Introduction

Like many other physical and biological processes, epidemics can be modelled mathematically. Epidemic mathematical modelling is important, not only to understand the disease progression, but also to provide predictions about the epidemics evolution and insights about the dynamics of the transmission rate and the effectiveness of control measures. There are several compartmental models in epidemiology, like the *SI*, *SIR*, *SICA* and the *SEIR* model, see, e.g., [3, 14, 28] and references cited therein. In this chapter, we consider the *SEIR* model, where the human population is divided into four mutually exclusive compartments: susceptible *S*, latent *E*, infected *I*, and a recovered or removed (dead) *R*. We assume that the population is homogeneous and the various classes are uniformly mixed. We consider the case of constant total population *N*, that is, $S(t) + E(t) + I(t) + R(t) = N$ for every time t in the time window $t \in [0, T]$ under study. In this case, the fraction of individuals in each compartment is defined as $s = S/N$, $e = E/N$, $i = I/N$ and $r = R/N$. The balance condition becomes $s + e + i + r = 1$. The assumptions made about the transmission of the infection and incubation period are reflected in the equations and parameters [14] and are explained below. We consider the following parameters:

- transmission coefficient – β ;
- infectious rate – γ ;
- recovery rate – μ .

Then the *seir* model is given by the following system of ordinary differential equations:

$$\begin{cases} \frac{ds}{dt}(t) = -\beta s(t) i(t), \\ \frac{de}{dt}(t) = \beta s(t) i(t) - \gamma e(t), \\ \frac{di}{dt}(t) = \gamma e(t) - \mu i(t), \\ \frac{dr}{dt}(t) = \mu i(t), \end{cases} \quad (1)$$

represented graphically in the diagram of Figure 1. The term $\beta s i$ represents the gain

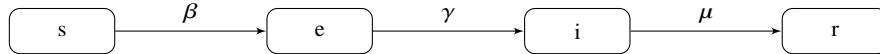


Fig. 1 Diagram of the compartmental model (1).

in the exposed class, which is proportional to the fraction of infective (and infectious) and susceptible individuals, where the transmission coefficient $\beta > 0$ is a constant parameter. Individuals are transferred from the susceptible class *s* to the exposed *e* at this rate $\beta s i$. The incubation period is of $1/\gamma$ days, with $\gamma > 0$, and after that time exposed individuals become infectious. The rate of removal of infective to the removed class is proportional to the number of infective, μi , with $\mu > 0$, where $1/\mu$ is a measure of the time spent in the infectious state [14].

The *seir* model (1) is an extension of the classical Kermack–McKendrick 1927 model [10, 11], where the class of exposed (latent) individuals is considered. SEIR type compartmental models have been extensively used to model the COVID-19 pandemic, see, e.g., [7, 22], and researchers have shown that it can describe the spread of COVID-19 in different countries: see [5] for a simulation of the COVID-19 spread in Lombardy (Italy) and also modifications of the SEIR model in [13, 17, 19]. Namely, in [13] three classes are added for confined, under quarantine and COVID-19 induced deaths. The model in [17] considers the age of the population, time delay on the development of the pandemic, and resusceptibility to COVID-19 with temporal immune response. An age-structured SEIR model is proposed in [19] considering 5-year bands until the age of 70 years and a single category aged 75 and older (resulting in 16 age categories for each class of individuals).

Optimal control theory is a branch of mathematics that involves finding optimal ways of controlling a dynamic system [6, 18]. Optimal control has been applied to epidemiological models for many different infectious diseases, such as HIV/AIDS, malaria, Ebola, tuberculosis and cholera [2, 12, 24, 27], and also non communicable diseases like cancer: see [21] and references cited therein.

Optimal control theory allows the study of the most cost-effective intervention strategy that changes the dynamics of a controlled system while minimizing a so-called objective function. In this chapter, we introduce two control functions in the *seir* model (1) that represent vaccination and plasma transfusion. Although vaccination has been widely studied from an optimal control point of view applied to epidemiological models, up to our knowledge, the plasma transfusion treatment has never been considered before. Plasma transfusion has been considered as a possible treatment for COVID-19, although it is still under study [1].

We propose five objective cost functionals and five corresponding optimal control problems for the three control systems that correspond to vaccination only, plasma transfusion treatment only, and combination of vaccination and plasma transfusion.

This chapter is organized as follows. In Section 2, the vaccination and plasma transfusion are introduced in the *seir* model, isolated and in combination, giving rise to three control systems that will be part of the optimal control problems proposed in Section 3. In Section 4, the solutions of the optimal control problems are compared numerically. We end with Section 5 of discussion and conclusions.

2 Control system: *seir* model with vaccination and plasma transfusion

In this section, in order to control the spread of the infection, two types of interventions are introduced into the *seir* model (1): vaccination u and plasma transfusion p . Instead of representing the vaccination and plasma transfusion by constant positive parameters, we assume that vaccination and plasma transfusion are given by two functions $u(\cdot)$ and $p(\cdot)$, respectively, that change in time and that modify the

dynamical behavior of model (1). In optimal control theory, functions $u(\cdot)$ and $p(\cdot)$ are usually called *controls*.

Starting by the vaccine, we introduce a control $u(\cdot)$ that represents the vaccination rate. By definition, it only makes sense to vaccinate people if they are susceptible to the disease. After being vaccinated, these people would become immune to the disease. In terms of the *seir* model states, this means that an individual in the s state would jump to the r state after being vaccinated. Thus, the model must be rewritten in the following way:

$$[\text{vaccination based control}] \quad \begin{cases} \frac{ds}{dt}(t) = -\beta s(t) i(t) - u(t) s(t), \\ \frac{de}{dt}(t) = \beta s(t) i(t) - \gamma e(t), \\ \frac{di}{dt}(t) = \gamma e(t) - \mu i(t), \\ \frac{dr}{dt}(t) = \mu i(t) + u(t) s(t), \end{cases} \quad (2)$$

where the control function $u(\cdot)$ is bounded between 0 and $u_{\max} \leq 1$.

Regarding treatment, the aim is to emulate a serological treatment, that is, a plasma transfusion. A plasma transfusion consists on infusing sick individuals with the blood plasma harvested from the immune individuals. Thus, in terms of the model, it requires that a recovered individual r donates plasma to an infectious individual i . The control is the rate at which this transfusion happens. Let the control be $p(\cdot)$. Then, the *seir* model (1) is rewritten in the following way:

$$[\text{plasma transfusion based control}] \quad \begin{cases} \frac{ds}{dt}(t) = -\beta s(t) i(t), \\ \frac{de}{dt}(t) = \beta s(t) i(t) - \gamma e(t), \\ \frac{di}{dt}(t) = \gamma e(t) - \mu i(t) - p(t) r(t) i(t), \\ \frac{dr}{dt}(t) = \mu i(t) + p(t) r(t) i(t), \end{cases} \quad (3)$$

where the control $p(\cdot)$ satisfies the control constraint $0 \leq p(\cdot) \leq p_{\max} \leq 1$.

Finally, the two previous controls are considered simultaneously, being the resulting model the following:

$$[\text{vaccination and plasma transfusion}] \quad \begin{cases} \frac{ds}{dt}(t) = -\beta s(t) i(t) - u(t) s(t), \\ \frac{de}{dt}(t) = \beta s(t) i(t) - \gamma e(t), \\ \frac{di}{dt}(t) = \gamma e(t) - \mu i(t) - p(t) r(t) i(t), \\ \frac{dr}{dt}(t) = \mu i(t) + p(t) r(t) i(t) + u(t) s(t). \end{cases} \quad (4)$$

The set of admissible controls functions is given by

$$\Omega = \left\{ (u(\cdot), p(\cdot)) \in (L^\infty(0, T))^2 \mid 0 \leq u(t) \leq u_{\max}, 0 \leq p(t) \leq p_{\max}, \forall t \in [0, T] \right\}. \quad (5)$$

3 Optimal control

Consider non-negative initial conditions for the state variables $(s, e, i, r) \in (R_0^+)^4$:

$$s(0) \geq 0, \quad e(0) \geq 0, \quad i(0) \geq 0, \quad r(0) \geq 0, \quad (6)$$

where the state variables satisfy $s(t)+e(t)+i(t)+r(t) = 1$, for all $t \in [0, T]$. In order to formulate an optimal control problem, a cost functional needs to be proposed, which in our case we intend to maximize. We propose an optimal control problem for the control systems given by (2), (3) or (4), with five different L^2 objective functionals, denoted for simplicity by $J_i, i = 1, \dots, 5$. All of them are obtained from

$$\mathcal{J}_\eta = \int_0^T \left(\eta_1 r(t) - \eta_2 i(t) - \eta_3 u^2(t) - \eta_4 p^2(t) \right) dt$$

as follows: $J_1 = \mathcal{J}_{(0,1,1,0)}$, $J_2 = \mathcal{J}_{(1,1,1,0)}$, $J_3 = \mathcal{J}_{(0,1,0,1)}$, $J_4 = \mathcal{J}_{(1,1,0,1)}$, and $J_5 = \mathcal{J}_{(0,1,1,1)}$. Other cases of cost functionals are obviously possible, but we found these five to be the most interesting. We also do not consider all possible combinations between the three control systems and the five costs to be maximized, restricting ourselves to five optimal control problems. Regarding the vaccination based control (2), we consider the two objective functionals

$$J_1(u(\cdot)) = \int_0^T \left(-i(t) - u^2(t) \right) dt \quad (7)$$

and

$$J_2(u(\cdot)) = \int_0^T \left(r(t) - i(t) - u^2(t) \right) dt. \quad (8)$$

When the cost functional is considered to be J_1 , the main goal of maximizing the functional is to minimize the fraction of infected individuals and, at the same time, the vaccination costs. We compare the solution to this optimal control problem with the one that maximizes J_2 , that is, the one that maximizes the fraction of recovered (immune) individuals and, simultaneously, minimizes the fraction of infected individuals and the vaccination costs. The numerical solutions are compared in Section 4.

When only the treatment by plasma transfusion is considered, that is, when we focus ourselves on the control system (3), we use the objective functionals J_3 and J_4 :

$$J_3(p(\cdot)) = \int_0^T \left(-i(t) - p^2(t) \right) dt, \quad (9)$$

$$J_4(p(\cdot)) = \int_0^T \left(r(t) - i(t) - p^2(t) \right) dt, \quad (10)$$

where maximizing J_3 corresponds to minimizing the fraction of infected individuals and the costs associated with plasma transfusion treatment, and for maximizing J_4

the main goal is to maximize the fraction of recovered individuals, by treatment, and, at the same time, minimize the fraction of infected individuals with less treatment cost as possible.

Finally, when both controls are considered simultaneously, modelled by the vaccination and plasma transfusion based control system (4), the objective functional considered to be maximized was J_5 :

$$J_5(u(\cdot), p(\cdot)) = \int_0^T \left(-i(t) - u^2(t) - p^2(t) \right) dt \quad (11)$$

with the main goal to minimize the fraction of infected individuals and the costs associated with vaccination and plasma transfusion treatment.

Associated to each of the cost functionals J_i , $i = 1, \dots, 5$, we propose an optimal control problem of determining the state trajectories $(s^*(\cdot), e^*(\cdot), i^*(\cdot), r^*(\cdot))$, associated to an admissible control $u^*(\cdot) \in \Omega$ and/or $p^*(\cdot) \in \Omega$ on the time interval $[0, T]$, satisfying one of the control systems (2)–(4), as explained, the initial conditions (6), and maximizing the corresponding functional. The five optimal control problems are denoted by (OC_i) , $i = 1, \dots, 5$, and are now summarized.

Vaccination based control system (2) and maximizing the cost functional J_1 :

$$J_1(u^*(\cdot)) = \max_{\Omega} \int_0^T \left(-i(t) - u^2(t) \right) dt. \quad (OC_1)$$

Vaccination based control system (2) and maximizing the cost functional J_2 :

$$J_2(u^*(\cdot)) = \max_{\Omega} \int_0^T \left(r(t) - i(t) - u^2(t) \right) dt. \quad (OC_2)$$

Plasma transfusion based control system (3) and maximizing the cost functional J_3 :

$$J_3(p^*(\cdot)) = \max_{\Omega} \int_0^T \left(-i(t) - p^2(t) \right) dt. \quad (OC_3)$$

Plasma transfusion based control system (3) and maximizing the cost functional J_4 :

$$J_4(p^*(\cdot)) = \max_{\Omega} \int_0^T \left(r(t) - i(t) - p^2(t) \right) dt. \quad (OC_4)$$

Vaccination and plasma transfusion control system (4) and maximizing the cost functional J_5 :

$$J_5(u^*(\cdot), p^*(\cdot)) = \max_{\Omega} \int_0^T \left(-i(t) - p^2(t) - u^2(t) \right) dt. \quad (OC_5)$$

Note that all optimal control problems have a L^2 -cost functional, in other words, the integrand of the cost J_i , $i = 1, \dots, 5$, is always convex with respect to the controls u and p . Moreover, the control systems (2)–(4) are Lipschitz with respect to the state variables (s, e, i, r) . These properties ensure the existence of an optimal control $(u^*(\cdot), p^*(\cdot))$ for the optimal control problems (OC_1) – (OC_5) . Moreover, we apply the Pontryagin Maximum Principle (see, e.g., [18]), which is a first order necessary optimality condition. The obtained result, here formulated and proved for the optimal control problem (OC_1) , can be trivially extended to the other optimal control problems (OC_i) , $i = 2, \dots, 5$.

Theorem 1 *The optimal control problem (OC_1) with fixed final time T admits a unique optimal solution $(s^*(\cdot), e^*(\cdot), i^*(\cdot), r^*(\cdot))$ associated to the optimal control $u^*(\cdot)$ given by*

$$u^*(t) = \min \left\{ \max \left\{ 0, \frac{(\lambda_4(t) - \lambda_1(t)) s(t)}{2} \right\}, u_{\max} \right\} \quad (12)$$

on $[0, T]$, where the adjoint functions λ_i satisfy

$$\begin{cases} \dot{\lambda}_1(t) = -\lambda_1(t) (-i(t) \beta - u(t)) - \lambda_2(t) i \beta - \lambda_4(t) u(t), \\ \dot{\lambda}_2(t) = \lambda_2(t) \gamma - \lambda_3(t) \gamma, \\ \dot{\lambda}_3(t) = 1 + \lambda_1(t) \beta s(t) - \lambda_2(t) \beta s(t) + \lambda_3(t) \mu - \lambda_4(t) \mu, \\ \dot{\lambda}_4(t) = 0, \end{cases} \quad (13)$$

with the transversality conditions $\lambda_i(T) = 0$, $i = 1, \dots, 4$.

Proof The existence of an optimal control $u^*(\cdot)$ of the optimal control problem (OC_1) is due to the convexity of the L^2 -cost functional J_1 and to the fact that the vaccinated based control system (2) is Lipschitz with respect to the state variables (s, e, i, r) : see, e.g., [6]. The uniqueness of the optimal control u^* comes from the boundedness of the state and adjoint functions and the Lipschitz property of system (2) (see [9, 26] and references cited therein). According to the Pontryagin Maximum Principle, if $u^*(\cdot)$ is optimal for the problem (OC_1) with fixed final time T , then there exists a nontrivial absolutely continuous mapping $\Lambda : [0, T] \rightarrow \mathbb{R}^4$, $\Lambda(t) = (\lambda_1(t), \lambda_2(t), \lambda_3(t), \lambda_4(t))$, called the *adjoint vector*, such that

$$\dot{s} = \frac{\partial H}{\partial \lambda_1}, \quad \dot{e} = \frac{\partial H}{\partial \lambda_2}, \quad \dot{i} = \frac{\partial H}{\partial \lambda_3}, \quad \dot{r} = \frac{\partial H}{\partial \lambda_4}$$

and

$$\dot{\lambda}_1 = -\frac{\partial H}{\partial s}, \quad \dot{\lambda}_2 = -\frac{\partial H}{\partial e}, \quad \dot{\lambda}_3 = -\frac{\partial H}{\partial i}, \quad \dot{\lambda}_4 = -\frac{\partial H}{\partial r},$$

where

$$\begin{aligned}
H &= H(s(t), i(t), c(t), a(t)) = -i(t) - u^2(t) \\
&\quad + \lambda_1(t) (-\beta s(t) i(t) - u(t) s(t)) \\
&\quad + \lambda_2(t) (\beta s(t) i(t) - \gamma e(t)) \\
&\quad + \lambda_3(t) (\gamma e(t) - \mu i(t)) \\
&\quad + \lambda_4(t) (\mu i(t) + u(t) s(t))
\end{aligned}$$

is the *Hamiltonian*, and the maximality condition

$$\begin{aligned}
H(s^*(t), e^*(t), i^*(t), r^*(t), \lambda^*(t), u^*(t)) \\
= \max_{0 \leq u \leq u_{\max}} H(s^*(t), e^*(t), i^*(t), r^*(t), \lambda^*(t), u(t))
\end{aligned}$$

holds almost everywhere on $[0, T]$. Moreover, the transversality conditions

$$\lambda_i(T) = 0, \quad i = 1, \dots, 4,$$

hold. Furthermore, from the maximality condition, we have

$$u^*(t) = \min \left\{ \max \left\{ 0, \frac{(\lambda_4(t) - \lambda_1(t)) s(t)}{2} \right\}, u_{\max} \right\}.$$

The proof is concluded. \square

To solve optimal control problems numerically, two approaches are possible: direct and indirect. Indirect methods are based on Pontryagin's Maximum Principle but not very much widespread since they are not immediately available by software packages. We refer the reader to [4] for the implementation of Pontryagin's Maximum Principle using Octave/MATLAB. Direct methods consist in the discretization of the optimal control problem, reducing it to a nonlinear programming problem [15, 20]. In the next section, we use the Applied Modeling Programming Language AMPL [8] to discretize the optimal control problems (OC_i) , $i = 1, \dots, 5$. Then, the resulting nonlinear programming problems are solved using the Interior-Point optimization solver developed by Wächter and Biegler [29], through the NEOS Server [16]. For more details on the numerical aspects see [25].

4 Numerical simulations and results

In this section, we provide numerical simulations for the solutions of the optimal control problems (OC_i) , $i = 1, \dots, 5$, proposed in Section 3. The following values for the initial conditions are considered:

$$s(0) = 0.88, \quad e(0) = 0.07, \quad i(0) = 0.05, \quad r(0) = 0, \quad (14)$$

and the parameter values

$$\beta = 0.3, \quad \gamma = 0.1887, \quad \mu = 0.1. \quad (15)$$

The initial conditions (14) were chosen arbitrarily, considering an hypothetical situation where 88% of the total population is susceptible to the disease and there is a relatively small percentage of infected population and no recovered individuals. The parameter values are chosen in such a way that model (1) simulates an epidemic outbreak, caused by a communicable disease. Moreover, we consider the control constraints with $u_{\max} = 0.5$ and $p_{\max} = 0.3$, that is, the admissible controls $(u, p) \in \Omega$ must satisfy $0 \leq u(t) \leq 0.5$ and $0 \leq p(t) \leq 0.3$ for all $t \in [0, T]$.

All computations have been performed with an Intel i7-4720HQ 2.60GHz processor, 8 GB of RAM, and an SSD disk of 128 GB under Windows 10, Home Edition of 64 bits.

4.1 The *seir* model without controls

The *seir* model differential equations were integrated using the ode45 MATLAB routine, which is based on an explicit Runge–Kutta method [23]. For the parameter values (15), the dynamic evolution of the uncontrolled system (1) is described in Figures 2–3. We observe that although the fraction of infected i and exposed e individuals tends to 0, after 100 units of time, more than 40 per cent of the population recovered or was removed (possible died from the disease).

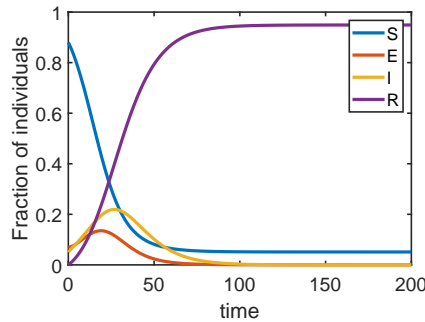


Fig. 2 Joint evolution of the state variables s , e , i and r of the uncontrolled model (1), during 200 time units.

These results were obtained in “real time” under MATLAB.

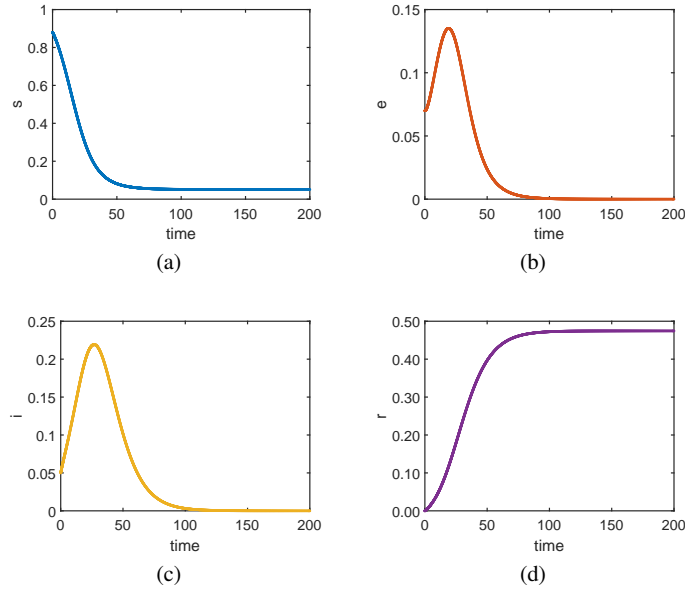


Fig. 3 Individual evolution of the state variables $seir$ of the uncontrolled model (1), during 200 time units. (a) susceptible state s . (b) exposed state e . (c) infected state i . (d) recovered state r .

4.2 The $seir$ model with controls

It is desirable to minimize the fraction of infected individuals that get infected by the disease with minimal costs.

4.2.1 Optimal control problems (OC_1) and (OC_2)

Firstly, we consider the effect of vaccinating the population at the first 20 time units, aiming at maximizing J_1 subject to the vaccination based control system (2), the initial conditions (14), and the control constraint $0 \leq u(t) \leq 0.5$. The results obtained are given in Figures 4 and 5.

We see that in both $seir$ evolutions, the susceptible s and recovered r states seem to interchange, as expected by the vaccination based control system (2). Further, looking at the vaccination control $u(\cdot)$ evolution, it is possible to see that in both Figures 4 and 5 its value starts at a maximum and then decays as time passes. This makes sense, since at the beginning of the epidemic there are more susceptible individuals s . Thus, it is expected that the rate of vaccination is larger at this time in order to try to vaccinate the most susceptible individuals s as possible before they start getting infected. Further, comparing the vaccination control of Figure 4 and Figure 5, one can see that applying the condition of maximizing the fraction of

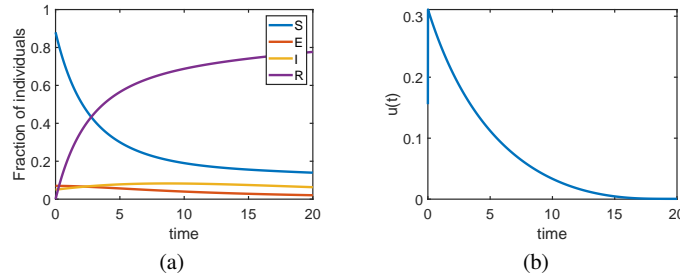


Fig. 4 Effect of vaccinating the population during 20 time units considering (OC_1) . (a) *seir* state variables applying vaccination. (b) Vaccination control $u(\cdot)$.

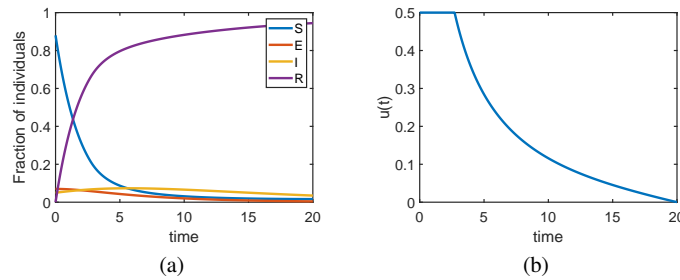


Fig. 5 Effect of vaccinating the population during 20 time units considering (OC_2) . (a) *seir* state variables applying vaccination. (b) Vaccination control $u(\cdot)$.

recovered individuals r with the cost functional J_2 translates into keeping the rate of vaccination at its maximum for 3 units of time before starting to decay with a less steeper slope than its analogue in J_1 .

4.2.2 Optimal control problems (OC_3) and (OC_4)

Regarding the plasma transfusion treatment, one can see that, in contrast to the vaccine control, here the control $p(\cdot)$ peaks later in time (see Figures 6 and 7). Again, this is something that makes sense since, in order for the treatment to be applied, there must be not only individuals in the infected i state, that are able to received the plasma, but also individuals in the recovered r state, that are able to donate the plasma. Evidently, these recovered individuals r must have been in the infected state i before.

Because this is an intervention that presupposes that the disease has evolved for some time, then a larger time window could allow one to visualize a stronger impact

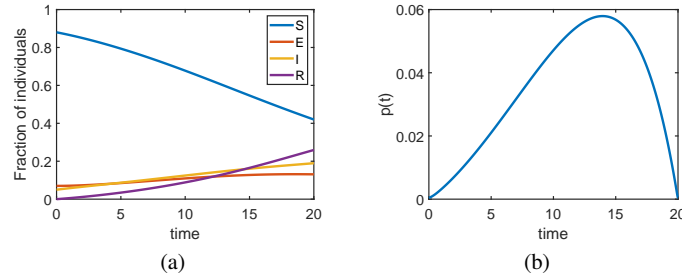


Fig. 6 Effect of infusing infectious individuals with plasma, during 20 time units, considering (OC_3) . (a) *seir* state variables applying plasma transfusion. (b) Plasma transfusion control $p(\cdot)$.

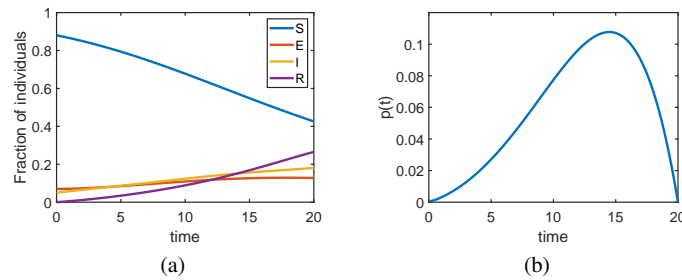


Fig. 7 Effect of infusing infectious individuals with plasma, during 20 time units, considering (OC_4) . (a) *seir* state variables applying plasma transfusion. (b) Plasma transfusion control $p(\cdot)$.

in the fractions of the i and r states. That said, a simulation for optimal control problems (OC_3) and (OC_4) is performed using $T = 100$.

The simulation that made the control increase the most with the time change was the one for the optimal control problem (OC_3) (Figure 8). Further, the control peak at Figure 8 also occurs before the control peak at Figure 9. This is expected since (OC_4) requires maximizing the r state, which implies again that more individuals must get into the i state so that they can get into the r state after recovering. It is also interesting to note that, according to the (OC_4) optimal control problem, one should not proceed with plasma transfusion to any infected individual during the beginning of the epidemic, in order to obtain the optimal control.

4.2.3 Optimal control problem (OC_5)

Finally, the combined effect of the two controls for the optimal control problem (OC_5) is presented in Figure 10. As expected, the peak of the vaccination rate occurs before the peak of the plasma transfusion rate. Apparently, the results in minimizing the

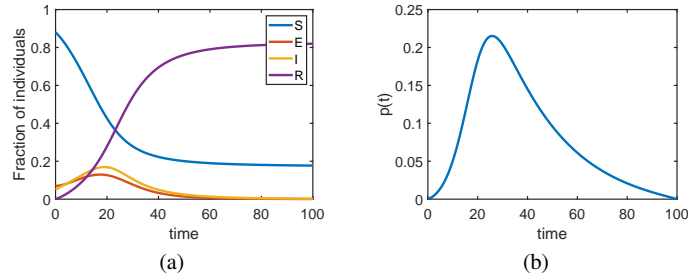


Fig. 8 Effect of infusing infectious individuals with plasma, during 100 time units, considering the cost functional J_3 . (a) *seir* state variables, applying plasma transfusion. (b) Plasma transfusion control $p(\cdot)$.

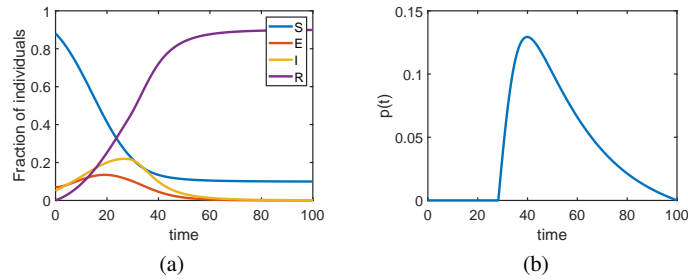


Fig. 9 Effect of infusing infectious individuals with plasma, during 100 time units, considering the cost functional J_4 . (a) *seir* state variables applying plasma transfusion. (b) Plasma transfusion control $p(\cdot)$.

fraction of individuals in the infected state i are better, when comparing Figure 10a with Figures 4a and 6a, but Figure 11 gives us a better understanding of the controls effects in the *seir* dynamics. Figure 11 shows the effect of the controls in the individual s , e , i , r states. Since the main objective of the control functionals is to minimize the number of individuals in the infected state i , then, by looking at Figure 11c, one can see that the control that minimizes the i fraction the most is the conjugation of both vaccination and plasma transfusion. This is also an intuitive result, since the vaccination makes more people jumping into the r state, which is the pool of individuals from where the plasma comes. On the other hand, the plasma transfusion by itself seems to be the less effective control in minimizing the infected fraction i (Figure 11c). This is expected since, as explained above, the plasma transfusion control needs more time to kick in the absence of a larger pool of recovered individuals r .

Furthermore, if the aim is to maximize the recovered state r or to minimize the susceptible s and exposed e states, then the vaccination is the best control (Figure 11d), a result also predicted by system (2). By analysing the control comparison

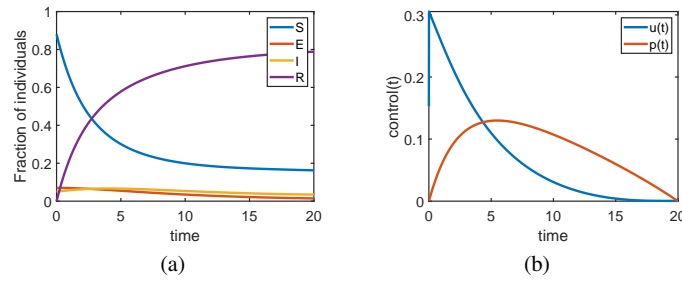


Fig. 10 Effect of both vaccinating susceptible individuals and infusing infectious individuals with plasma during 20 time units considering J_5 . (a) *seir* states applying vaccination and plasma transfusion. (b) Controls $u(t)$ and $p(t)$.

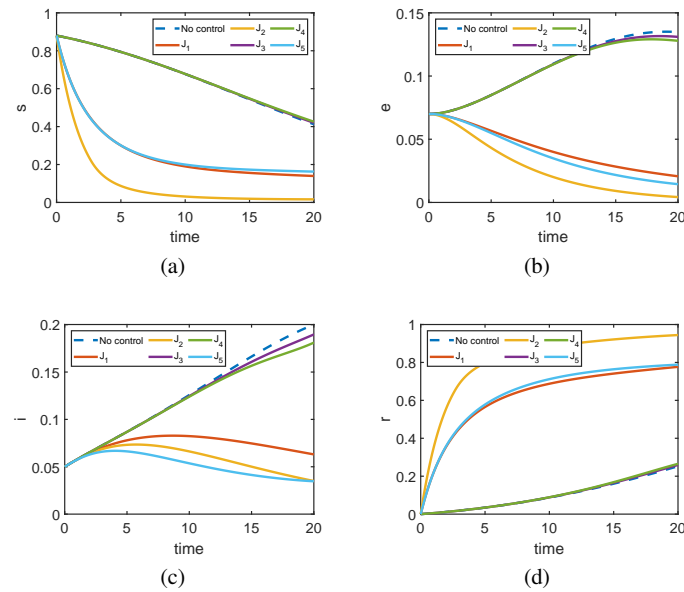


Fig. 11 Individual evolution of the controlled and uncontrolled states *seir*, during 20 time units. (a) susceptible state s . (b) exposed state e . (c) infected state i . (d) removed state r .

at Figure 12, one can see that the control that benefits the most with the combined approach of both vaccination and plasma transfusion is the plasma control. This can be explained since one can think that if we apply vaccination in the beginning of the epidemics, then the fraction of recovered individuals r increases faster, providing a bigger substract to do plasma transfusion sooner and at a higher rate.

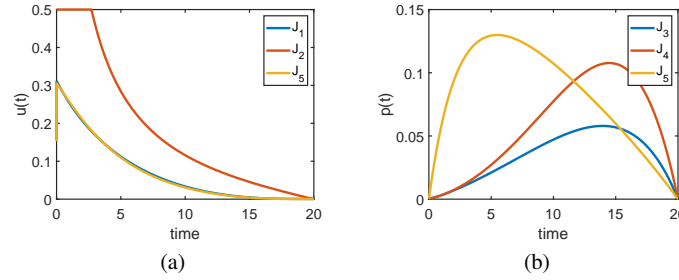


Fig. 12 Evolution of vaccination and plasma transfusion controls, during 20 time units. (a) Vaccination control $u(\cdot)$. (b) Plasma transfusion control $p(\cdot)$.

All the optimal control simulations were carried out using NEOS Server 6.0, their duration varying between 0.508 and 1.149 seconds, for 20 units of time, and between 24.431 and 30.702 seconds, for 100 units of time.

5 Discussion and conclusion

The *seir* model (1) was solved numerically in both uncontrolled and controlled conditions. Of the controls employed, the combined action of vaccination and plasma transfusion seems to have the higher impact in reducing the fraction of infectious individuals. Moreover, the plasma transfusion acquires a more important role as the fraction of individuals in the recovered state increases, which explains why whether joining the vaccination or increasing the duration of the simulations leads to an higher peak of the plasma transfusion rate. In fact, by joining the vaccination, one can not only increase the plasma transfusion rate peak but also anticipate it.

To sum up, controls can act at different timings of the epidemics dynamics and one control can be more adequate in the beginning of the epidemic whilst other might be more appropriated in a later state.

Code availability

The code is available from the authors on request.

Acknowledgements This research was partially supported by the Portuguese Foundation for Science and Technology (FCT) within “Project n. 147 – Controlo Ótimo e Modelação Matemática da Pandemia COVID-19: contributos para uma estratégia sistémica de intervenção em saúde na comunidade”, in the scope of the “RESEARCH 4 COVID-19” call financed by FCT. The work of Silva and Torres was also partially supported within project UIDB/04106/2020 (CIDMA). Moreover,

Silva is also supported by national funds (OE), through FCT, I.P., in the scope of the framework contract foreseen in the numbers 4, 5 and 6 of the article 23, of the Decree-Law 57/2016, of August 29, changed by Law 57/2017, of July 19. The authors are grateful to two anonymous reviewers for helpful comments and suggestions.

References

1. American Society of Hematology, COVID-19 and Convalescent Plasma: Frequently Asked Questions, <https://www.hematology.org/covid-19/covid-19-and-convalescent-plasma>
2. Area, I., Ndaïrou, F., Nieto, J.J., Silva, C.J. and Torres, D.F.M.: Ebola Model and Optimal Control with Vaccination Constraints, *J. Ind. Manag. Optim.* **14**, no. 2, 427–446 (2018). arXiv:1703.01368
3. Brauer, F. and Castillo-Chavez, C.: *Mathematical Models in Population Biology and Epidemiology*, Texts in Applied Mathematics, Springer New York (2011)
4. Campos, C., Silva, C.J. and Torres, D.F.M.: Numerical Optimal Control of HIV Transmission in Octave/MATLAB, *Math. Comput. Appl.* **25**, no. 1, 20 pp (2020). arXiv:1912.09510
5. Carcione, J.M., Santos, J.E., Bagaini, C. and Ba, J.: A Simulation of a COVID-19 Epidemic Based on a Deterministic SEIR Model, *Front. Public Health* 8:230 (2020).
6. Cesari, L. *Optimization – Theory and Applications*. Problems with Ordinary Differential Equations, Applications of Mathematics 17, Springer-Verlag, New York, 1983.
7. COVID-19 Projections Using Machine Learning, <https://covid19-projections.com>
8. Fourer, R., Gay, D.M. and Kernighan, B.W.: *AMPL: A Modeling Language for Mathematical Programming*, Duxbury Press, Brooks–Cole Publishing Company, 1993.
9. Jung, E., Lenhart, S., Feng, Z.: Optimal control of treatments in a two-strain tuberculosis model, *Discrete Contin. Dyn. Syst. Ser. B* **2** (4), 473–482 (2002).
10. Kermack, W.O. and McKendrick, A.G.: A Contribution to the Mathematical Theory of Epidemics, *Proc. Roy. Soc. Lond. A* **115**, 700–7–21 (1927).
11. Kermack, W.O., McKendrick, A.G. Contributions to the mathematical theory of epidemics I. *Bltm Mathcal Biology* **53**, 33–55 (1991).
12. Lemos-Paião, A.P., Silva, C.J., Torres, D.F.M. and Venturino, E.: Optimal Control of Aquatic Diseases: A Case Study of Yemen’s Cholera Outbreak, *J. Optim. Theory Appl.* **185**, no. 3, 1008–1030 (2020). arXiv:2004.07402
13. López, L. and Rodó, X.: A Modified SEIR Model to Predict the COVID-19 Outbreak in Spain and Italy: Simulating Control Scenarios and Multi-Scale Epidemics, Available at SSRN: <http://dx.doi.org/10.2139/ssrn.3576802>
14. Murray, J.D.: *Mathematical Biology*, Springer Berlin Heidelberg (2013)
15. Nematì, S.; Lima, P.M.; Torres, D.F.M. A numerical approach for solving fractional optimal control problems using modified hat functions. *Commun. Nonlinear Sci. Numer. Simul.* **78** (2019), Art. 104849, 14 pp. arXiv:1905.06839
16. NEOS Interfaces to Ipopt, <https://neos-server.org/neos/solvers/nco:Ipopt/AMPL.html>.
17. Ng, K. Y. and Gui, M. M.: COVID-19: Development of a robust mathematical model and simulation package with consideration for ageing population and time delay for control action and resusceptibility. *Physica D. Nonlinear phenomena*, **411**, 132599 (2020).
18. Pontryagin, L., Boltyanskii, V., Gramkrelidze, R. and Mischenko, E. *The Mathematical Theory of Optimal Processes*, Wiley Interscience, 1962.
19. Prem, K. et. al.: The effect of control strategies to reduce social mixing on outcomes of the COVID-19 epidemic in Wuhan, China: a modelling study, *The Lancet Public Health*, **5** (5), e261–e270 (2020).
20. Salati, A.B.; Shamsi, M.; Torres, D.F.M. Direct transcription methods based on fractional integral approximation formulas for solving nonlinear fractional optimal control problems. *Commun. Nonlinear Sci. Numer. Simul.* **67** (2019) 334–350. arXiv:1805.06537

21. Schättler, H. and Ledzewicz, U., *Optimal Control for Mathematical Models of Cancer Therapies, An Application of Geometric Methods*, Springer-Verlag New York, 2015.
22. SEIR Model for the COVID-19 Epidemic, <https://www.comsol.pt/model/seir-model-for-the-covid-19-epidemic-86511>.
23. Shampine, L.F. and Reichelt, M. W.: The MATLAB ODE Suite, *SIAM Journal on Scientific Computing* **18**, 1–22 (1997).
24. Silva, C.J. and Maurer, H.: Optimal control of HIV treatment and immunotherapy combination with state and control delays, *Optim Control Appl. Meth.* **41**, 537–554 (2020).
25. Silva, C.J., Maurer, H. and Torres, D.F.M.: Optimal control of a tuberculosis model with state and control delays, *Math. Biosci. Eng.* **14**, no. 1, 321–337 (2017). [arXiv:1606.08721](https://arxiv.org/abs/1606.08721)
26. Silva, C.J., Torres, D.F.M.: Optimal control for a tuberculosis model with reinfection and post-exposure interventions, *Math. Biosci.* **244**, no. 2, 154–164 (2013). [arXiv:1305.2145](https://arxiv.org/abs/1305.2145)
27. Silva, C.J. and Torres, D. F. M.: A TB-HIV/AIDS coinfection model and optimal control treatment, *Discrete Contin. Dyn. Syst.*, **35**, no. 9, 4639–4663 (2015). [arXiv:1501.03322](https://arxiv.org/abs/1501.03322)
28. Silva, C. J. and Torres, D. F. M.: On SICA models for HIV transmission. In: *Mathematical Modelling and Analysis of Infectious Diseases*, ed. by K. Hattaf and H. Dutta., *Studies in Systems, Decision and Control* 302 (2020), Springer Nature Switzerland, 2020, 155–179. [arXiv:2004.11903](https://arxiv.org/abs/2004.11903)
29. Wächter, A. and Biegler, L. T.: On the implementation of an interior-point filter line-search algorithm for large-scale nonlinear programming, *Math. Program.* **106**, 25–57 (2006).